THE JOURNAL OF PHYSICAL CHEMISTRY C

Article

pubs.acs.org/JPCC

Solvent-Independent Electrode Potentials of Solids Undergoing Insertion Electrochemical Reactions: Part I. Theory

Antonio Doménech-Carbó*

Departament de Química Analítica, Facultat de Química, Universitat de València, Dr. Moliner 50, 46100 Burjassot, Valencia, Spain

ABSTRACT: A formally solvent-independent redox system can be theoretically defined using the Lovric and Scholz modeling of the voltammetry of microparticles for ion-insertion solids. The proposed theory is based on the extra-thermodynamic assumptions that no net charge accumulates at the solidlelectrolyte interface and the assumption that the structure of the solid and the ion binding remain unaffected by the solvent. Under voltammetric conditions, the corresponding redox potential can be estimated from voltammetric and chronoamperometric data assuming electrochemical reversibility and diffusive charge transport in the solution and solid phases, also taking into account ion partition (electrolyte/solid) and ion-binding equilibria.

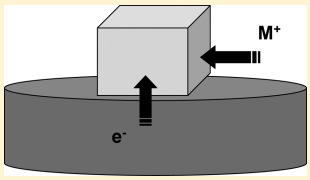

INTRODUCTION

Correlation between electrochemical measurements in different solvents requires, in order to obtain thermodynamic quantities, defining a solvent-independent scale of standard redox potentials.[1] This problem, first formulated by Bjerrum and Larsson,[2] involves the determination of liquid junction potentials, which, unfortunately, means spinning around: the determination of junction potentials requires the disposal of a solvent-independent redox potential scale, while, conversely, such scale would be available after determining the junction potentials. This problem cannot be solved on the basis of strict thermodynamics, so that extra-thermodynamic assumptions have been used to determine junction potentials.[3−7]

Operationally, three main approaches have been used to avoid the liquid junction potential problem. First, it is assumed that liquid junction potentials are negligible (or become compensated) when a salt bridge composed of a salt of a quasi-spherical cation and a quasi-spherical anion of about the same size is used. In the second approach, a supporting electrolyte is used whose cations and anions are assumed to have similar electrochemical mobilities and equal solvation Gibbs energies in different solvents. In the first case, picrate salt bridges (Et_4Npic) are typically used,[8] whereas in the second case, tetraphenylarsonium[9] or tetraphenylphosphonium[10,11] tetraphenylborates are usually employed. A third operational approach is based on using an electrochemical couple whose electrode potential is assumed to be solvent-independent. The redox couples recommended by the IUPAC are ferrocenium ion/ferrocene or bis(η-biphenyl)chromium(I)/bis(biphenyl)-chromium(0) ($BBCr^+$/BBCr).[1,12,13]

The last approach is based, strictly, on the assumption that the difference in the solvation Gibbs energies for the oxidized and reduced for of the redox couple is the same in all solvents. This means that, in fact, the above problems are directly related to that of determining thermodynamic quantities for single ions. Again, extrathermodynamic assumptions have to be introduced, usually combining quantum mechanical calculations to describe the solvent portion in the vicinity of the ion and classical continuum modeling to describe the behavior of the solvent in regions relatively far from the ion.[14−25] Obtaining experimental data from direct polarization of liquid/liquid interfaces with two adjacent electrolyte-supported immiscible liquids,[26] membrane-modified liquid−liquid interfaces,[27,28] large surface area,[29] micro/nanohole,[30−33] and triple-phase boundary measurements at microdroplets immobilized on electrode surfaces[34−38] has been recently described.

In prior works the voltammetry of microparticles (VMP) methodology, a solid-state technique developed by Scholz et al.,[39,40] has been applied to determine individual Gibbs energies of transfer of cation[41] and anion[42,43] between two miscible solvents. In this report, a theoretical modeling is proposed that is potentially usable to define solvent-independent redox systems combining voltammetric and chronoamperometric measurements on selected ion-insertion solids. The model only requires Nernstian electrochemical behavior and solving the diffusion problem in terms of Fick's laws. This formulation derives from those for the electrochemistry of ion-insertion solids[44−49] and redox polymers[50−52] with account of partition[53] and binding[54] equilibria (for details concerning the thermodynamics of ion partition equilibrium between two phases, see[55,56]). Application of this method to define solvent-independent potentials involves two extra-thermodynamic assumptions: (i) there is no accumulation of net charge in the solid complex/electrolyte boundary and (ii) the structures of the solid and the ion binding to the solid are not affected by the solvent. Prior data on the solid-state electrochemistry of Prussian Blue[41] and alkynyl−diphosphine dinuclear Au(I) complexes and heterometallic Au(I)−Cu(I) cluster complexes containing ferrocenyl units[42,43] make such systems reasonable candidates for making the proposed method operative.

THEORY

Solvation Problem. Figure 1 illustrates the thermochemical cycle for correlating equilibrium electrode potentials with

Received: September 10, 2012
Published: November 13, 2012

   dx.doi.org/10.1021/jp308966w | J. Phys. Chem. C 2012, 116, 25977−25983

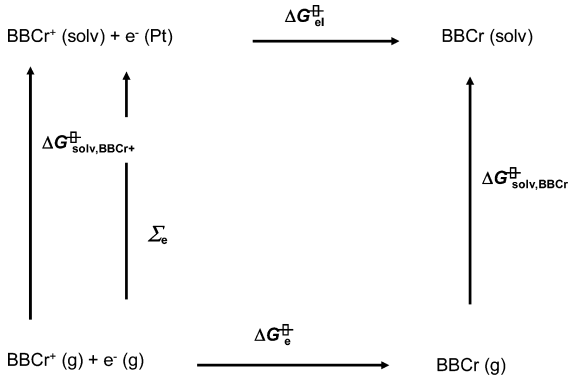

Figure 1. Thermochemical cycle for the reduction of the $BBCr^+/BBCr$ couple in different solvents using a Pt base electrode.

different Gibbs free energies in the case of the $BBCr^+/BBCr$ couple.

$$\Delta G_{el}^{\ominus} = \Delta G_{e}^{\ominus} + \Delta G_{solv,BBCr}^{\ominus} - \Delta G_{solv,BBCr^+}^{\ominus} - \Sigma_e \quad (1)$$

Here the Gibbs energy of the electrochemical reduction of the complex, $\Delta G_{el}^{\ominus}$, is related to the corresponding quantity for the complex in the gas phase, $\Delta G_{el}^{\ominus}$, the Gibbs energy of solvation of the oxidized and reduced forms of the complexes $\Delta G_{solv,BBCr^+}^{\ominus}$ and $\Delta G_{solv,BBCr}^{\ominus}$, respectively, and the Gibbs energy of the electron transfer from the gas phase to the base electrode, $\sum_e$. Combining the expressions for two different solvents, s1 and s2, one obtains:

$$\Delta G_{el}^{\ominus}(s2) - \Delta G_{el}^{\ominus}(s1) = \Delta G_{BBCr,s1\rightarrow s2}^{\ominus} - \Delta G_{BBCr^+,s1\rightarrow s2}^{\ominus} \quad (2)$$

$\Delta G_{BBCr,s1\rightarrow s2}^{\ominus}$ and $\Delta G_{BBCr^+,s1\rightarrow s2}^{\ominus}$ are the Gibbs energies of transfer of BBCr and $BBCr^+$ from the solvent s1 to the solvent s2, defined as the difference between the respective solvation Gibbs energies in such solvents. Strictly, this redox system would be solvent-independent if the Gibbs energies of transfer of BBCr and $BBCr^+$ from the solvent s1 to the solvent s2 are equal and thus compensate.

Defining a Solvent-Independent Redox Potential. Let us consider a microparticulate deposit of an ion-insertion solid on an inert electrode being in contact with an electrolyte containing monovalent (for simplicity) M^+ and An^- ions, as schematically shown in Figure 2. It is assumed that the solid contains immobile redox centers L, which can change reversibly their oxidation state by means of an *n*-electron transfer process. Charge conservation requires that the reduction of the immobile redox centers is coupled to the ingress of cations (or expulsion of anions) from the electrolyte into the solid lattice. Oxidation of L will be coupled to an expulsion of cations (or ingress of anions). The electrochemical reduction (oxidation) of the solid material can be assumed to start at the three-phase boundary electrode|solid particle|electrolyte and to propagate through the solid via electron hopping between immobile redox centers and ion diffusion within the solid, a situation that can be represented in terms of diffusion of electrons and ions in mutually perpendicular directions. The overall redox equilibrium of a solid with the composition $\{L^{m+}\cdots m An^-\}_{solid}$ can be described by the following equation when cation insertion is assumed to provide the charge compensation:

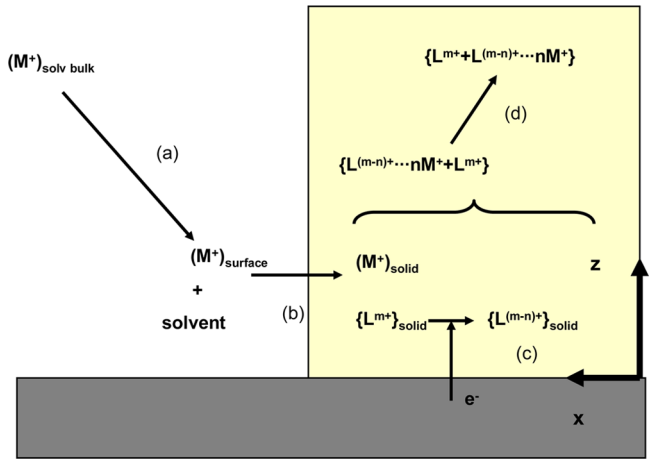

Figure 2. Schematic representation of formal processes represented by eqs 4−7 based on the Lovric and Scholz modeling[45,48] of the electrochemistry of ion-insertion solids. (a) Diffusion of M^+ from bulk to solid|electrolyte interface, (b) ion transfer with desolvation, (c) electron transfer at the electrode|solid interface, and (d) coupled ion−electron diffusion in solid.

$$\{L^{m+}\cdots m An^-\}_{solid} + nM^+_{solution} + ne^- \rightleftarrows \{L^{(m-n)+}\cdots nM^+\cdots m An^-\}_{solid} \quad (3)$$

The reduction and oxidation processes described by eq 3 can be formally separated into four processes: (i) diffusion of solvated ions from the solution bulk to the particle|electrolyte interface, (ii) ion desolvation at the particle surface and ion transfer to the solid, (iii) electron transfer to/from the immobile redox centers, and (iv) coupled diffusion of ions and electrons (electron hopping) in the solid. Such processes can be represented by means of the following equations (for brevity, only reduction is considered here):

$$(M^+_{solution})_{bulk} \xrightarrow{\text{diffusion}} (M^+_{solv})_{surf} \quad (4)$$

$$(M^+_{solv})_{surf} \xrightarrow{\text{ion transfer}} \{M^+\}_{solid} + \text{solvent} \quad (5)$$

$$\{L^{m+}\}_{solid} + ne^- \xrightarrow{\text{electron transfer}} \{L^{(m-n)+}\}_{solid} \quad (6)$$

$$n\{M^+\}_{solid} + \{L^{(m-n)+}\}_{solid} \xrightarrow{\text{binding}} \{L^{(m-n)+}\cdots nM^+\}_{solid} \quad (7)$$

$$\{L^{(m-n)+}\cdots nM^+ + \bar{L}^{m+}\}_{solid} \xrightarrow{\text{coupled electron−ion diffusion}} \{L^{m+} + \bar{L}^{(m-n)+}\cdots nM^+\}_{solid} \quad (8)$$

$\bar{L}$ just means another redox center.

An schematic representation of the above processes is depicted in Figure 2, based on the Lovric and Scholz modeling[46,48] of the electrochemistry of ion-insertions solids. Equations 4 and 5 represent, conjointly, the partition process, for which an equilibrium constant, K_{pt}, can be defined as $K_{pt} = a_{M^+_{solid}}/a_{M^+_{solution}}$, where $a_{M^+_{solid}}$ denotes the activity of the M^+ ion in the solid particle and $a_{M^+_{solution}}$ is the activity of that ion in the electrolyte solution.

Equation 7 represents the binding equilibrium between the immobile redox centers of the solid (in its reduced form) and the counterions, in turn represented by a binding equilibrium constant, K_{bd}, which can be defined as $K_{bd} = a_{LM}/(a_L a^n_{M^+_{solid}})$, where a_{LM} and a_L denote, respectively, the activity of the

dx.doi.org/10.1021/jp308966w | J. Phys. Chem. C 2012, 116, 25977−25983

$\{L^{(m-n)+}\cdots nM^+\}_{solid}$ and $\{L^{(m-n)+}\}_{solid}$ species. It should be noted that such processes are necessarily coupled by reasons of charge conservation so that their separation is only formal.

Importantly, eq 6 can be viewed as a "pure" solid-state reduction with a standard redox potential, $E^{\ominus}_{L^{m+/(m-n)+}}$. We are aware of the involved problems with the above definitions, especially (i) that eqs 6 and 7, although written separately, correspond to an unique process by obvious reasons of charge conservation, and (ii) the fact that there is not yet a possibility to define and determine the activities of the involved species in the solid. In equilibrium, the composition of the solid phase is determined by the electrode potential according to the Nernst equation so that, adapting the treatment of Scholz et al.[45,46,57] to describe reversible solid-state electrochemistry of ion-insertion solids, the midpeak potential measured in cyclic voltammetric experiments should satisfy the relationship:

$$E_{mp}(LM/L) = E^{\circ}_{L^{m+/(m-n)+}} + \frac{RT}{nF}\ln K + \frac{RT}{nF}\ln\left(\frac{a_{LM}}{a_L}\right) + \frac{RT}{F}\ln a_{M^+_{solution}} \quad (9)$$

In this equation, $E^{\ominus}_{L^{m+/(m-n)+}}$ represents the standard potential for the redox process described by eq 6, $a_{M^+_{solution}}$ is the activity of the M^+ ions in the electrolyte bulk, and a_{ML} and a_L are the thermodynamic activities of the oxidized and reduced forms of the solid. This treatment is equivalent to the generalized description of the thermodynamics of three-phase electrodes from Hermes and Scholz.[58] Notice that in the above equation the diffusion term which, strictly, correlates formal potentials with midpeak potentials,[59] is taken, as usual, as unit.

In eq 9, K denotes the equilibrium constant for the reaction:

$$\{L^{(m-n)+}\} + nM^+(solution) \rightarrow \{L^{(m-n)+} + nM^+\} \quad (10)$$

This equation can be obtained as the sum of reactions described by eqs 4, 5, and 7, so that $K_{bd} = a_{LM}/(a_L a^n_{M^+_{solution}}) = [a_{LM}/(a_L a^n_{M^+_{solid}})][a_{M^+_{solid}}/(a_{M^+_{solution}})]^n = K_{bd}K^n_{pt}$.

As previously described, K_{pt} represents the equilibrium constant for the ion partition equilibrium, which can be described by the sum of eqs 4 and 5, whereas K_{bd} denotes the binding equilibrium constant for the process represented by eq 7, which formally precludes the process of coupled ion-electron diffusion described by eq 8.

The central idea is that although $E^{\ominus}_{L^{m+/(m-n)+}}$ cannot be directly measured separately from K, this nominally solvent-independent potential could be calculated from voltammetric data upon estimating K. For this last purpose, chronoamperometric data could be used, as described in the next section.

Diffusion Problem: Microparticulate Deposit. For this purpose, let us first consider the 2-D scheme for microparticulate deposits (see Figure 2) used by Schröder et al.[49], where it is assumed that: (i) charge-balancing cations M^+ enter the solid only in the x direction, starting in the vicinity of the three-phase solid/electrode/electrolyte junction, (ii) electrons flow across the electrode/particle interface only in the z direction, and (iii) the concentrations of the oxidized and reduced centers at the three-phase junction are thermodynamically governed.

In this approach, charge transport is determined by both the electron diffusion in the z direction and ion diffusion in the x direction, Fick's law being:

$$\frac{\partial c_{LM}(x,z,t)}{\partial t} = D_{M^+_{solid}}\frac{\partial^2 c_{LM}(x,z,t)}{\partial x^2} + D_e\frac{\partial^2 c_{LM}(x,z,t)}{\partial z^2} \quad (11)$$

Here $D_{M^+_{solid}}$ and D_e represent, respectively, the diffusion coefficients for cations and electrons in the solid. Assuming that the time of the experiment is sufficiently short to ensure that the diffusion−migration layer thickness is small as compared with the thickness of the solid, the problem can be described in terms of the usual semi-infinite boundary conditions (vide infra). The model of Schröder et al.[49] predicts that for a deposit of N cuboid particles containing immobile redox centers in concentration c_L displaying a reversible n-electron oxidation process, in contact with an electrolyte solution containing a large concentration of M^+ cations, the chronoamperometric current at short times is given by:

$$i = nNFc_L\left[p\left(\left(\frac{\Delta z D_e^{1/2} + \Delta x D_{M^+_{solid}}^{1/2}}{2\pi^{1/2}t^{1/2}}\right) + (D_e D_{M^+_{solid}})^{1/2}\right) - 4D_{M^+_{solid}}(2D_e t)^{1/2}\right] \quad (12)$$

In this equation, p represents the perimeter of the electrode/crystal interface and Δx and Δz, represent the size of the discrete boxes in which the crystal is divided for numerical simulation procedures. The model can be extended to the 3-D situation schematized in Figure 3, resulting in similar theoretical

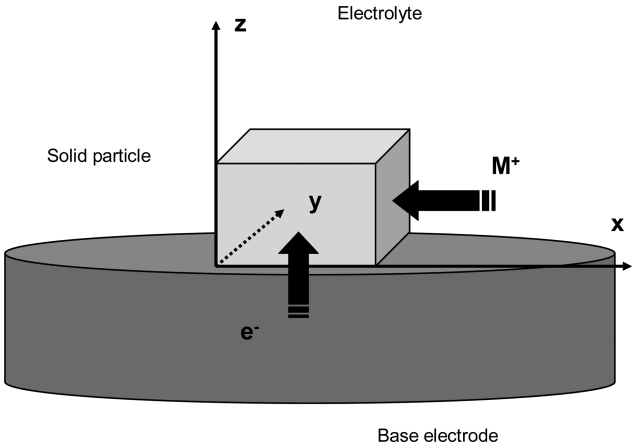

Figure 3. Schematic representation of the microparticulate deposit of an ion-insertion solid on an inert electrode described in Schröder et al.[49]

expressions when equal cation diffusion exists in the x and y directions. The first term of the above equation corresponds to a Cottrell-type behavior (i proportional to $t^{-1/2}$), whereas the second and third terms are associated, respectively, with effects due to the finite size of the crystals and the edge/corner constraints on charge diffusion. Interestingly, plots of $it^{1/2}$ versus t should exhibit a maximum at a transition time t_{max} given by:

$$t_{max} = \frac{p^2}{128D_{M^+_{solid}}} \quad (13)$$

The $it^{1/2}$ product at this time, $(it^{1/2})_{max}$, is:

dx.doi.org/10.1021/jp308966w | J. Phys. Chem. C 2012, 116, 25977−25983

$$(it^{1/2})_{max} = nNFc_1 p\left[\frac{\Delta z D_e^{1/2} + \Delta x D_{M^+_{solid}}^{1/2}}{2\pi^{1/2}} + pD_e^{1/2}\left(\frac{\sqrt{128} - 4\sqrt{2}}{128}\right)\right] \quad (14)$$

Interestingly, $D_{M^+_{solid}}$ can be directly calculated from chronoamperometric data using eq 13 provided that p is known. This parameter can be reasonably estimated, under determined circumstances, from electron microscopy data.[60]

Diffusion Problem: Homogeneous Solid Film. Application of the foregoing modeling to microparticulate deposits of the systems studied here is made difficult by the involved 3-D geometry (diffusion of electrons and anions through the solid occur in perpendicular directions) and the constraints introduced by the limited particle size.[49] Under most conditions, however, this situation can be described by representing the microparticulate deposit as a cylinder, of thickness δ, of the ionically and electronically conducting solid, pressed on the inert electrode in such a way that only a circular surface of the cylinder is exposed to the solution, as schematized in Figure 4.[46,53,61,62] Qualitatively, one can assume

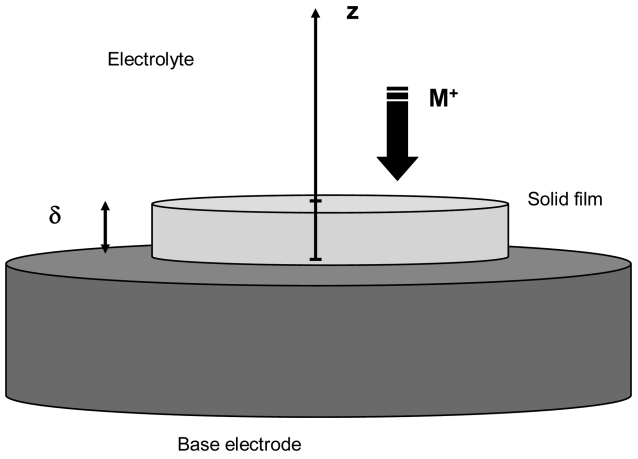

Figure 4. Schematic representation of a cylinder of an ion-insertion solid placed on an inert electrode following Lovric et al.[46] and Bard et al.[53]

that in a CA experiment at a potential sufficiently negative (reduction) or positive (oxidation) to ensure diffusion-controlled conditions, the electrolyte ions permeate progressively the solid. At short times and high ion concentration in the electrolyte, the mobile ions permeate the film from the solid−electrolyte interface so that the CA response will be mainly due to ion diffusion through the solid. Under these circumstances, the behavior described by eqs 12 and 14 would be operative. At longer times and relatively low concentration of anions in the electrolyte, the diffusion layer tends to be confined to the solution phase, and the current will be increasingly controlled by the diffusion of ions in the same. The diffusion of cations into a solid film where immobile redox centers are reversibly reduced would formally be equivalent to electroactive species diffusion in a redox polymer when the diffusion rate of cations rather than electron hopping between redox centers becomes rate-determining. Here, assuming mass transfer by diffusion in both the electrolyte and the solid film phases, the diffusion problem can be reduced to 1-D diffusion between two phases. It will be assumed that electron diffusion is faster than cation diffusion so that cation diffusion is determining the rate of the overall process. This is an oversimplification because coupled ion transport and electron transport needs to be modeled. Then, Fick's law governing charge diffusion in the solid and the solution can be written as:

$$D_{M^+_{solid}}\left(\frac{\partial^2 c_{M^+_{solid}}(z,t)}{\partial z^2}\right) = \frac{\partial c_{M^+_{solid}}(z,t)}{\partial t}, \quad 0 < z < \delta \quad (15)$$

$$D_{M^+_{solution}}\left(\frac{\partial^2 c_{M^+_{solution}}(z,t)}{\partial z^2}\right) = \frac{\partial c_{M^+_{solution}}(z,t)}{\partial t}, \quad \delta < z < \infty \quad (16)$$

with $D_{M^+_{solution}}$ and $D_{M^+_{solid}}$ being, respectively, the diffusion coefficients of cations in the electrolyte solution and in the solid. In these equations, $c_{M^+_{solution}}(z,t)$ represents the concentration of free cations in the electrolyte at a distance z from the electrolyte/crystal interface at a time t. The initial conditions are:

$$c_{M^+_{solid}}(z,0) = 0, \quad 0 < z < \delta \quad (17)$$

$$c_{M^+_{solution}}(z,0) = c_{M^+_{solution}}, \quad \delta < z < \infty \quad (18)$$

The system can be taken as semiinfinite in the solution phase so that the boundary conditions are:

$$c_{M^+_{solid}}(0,t) = 0 \quad (19)$$

$$\lim_{z\to\infty} c_{M^+_{solution}}(z,t) = c_{M^+_{solution}} \quad (20)$$

The continuity in the flux of material across the electrolyte-solid film interface is given by:

$$\left(D_{M^+_{solid}}\frac{\partial c_{M^+_{solid}}(x,t)}{\partial z}\right)_{x=\delta} = \left(D_{M^+_{solution}}\frac{\partial c_{M^+_{solution}}(z,t)}{\partial z}\right)_{z=\delta} \quad (21)$$

To describe the flux of anions through the electrolyte−solid film interface, it will be assumed that the desolvation process described by eq 4 and the subsequent ingress of cations in the solid phase are sufficiently fast so that they can be treated, following Bard et al.,[53] as a partitioning equilibrium, characterized by the partition equilibrium constant, K_{pt}, previously defined. Accordingly, the cation concentration in the solid at the film−solution interface, $c_{M^+_{solid}}(\delta,t)$, will be related to its concentration in the solution at that interface, $c_{M^+_{solution}}(\delta,t)$, by means of the relationship:

$$c_{M^+_{solid}}(\delta,t) = K_{ex} c_{M^+_{solution}}(\delta,t) \quad (22)$$

Solving the diffusion problem leads to the following current−time chronoamperometric response under diffusion-controlled conditions:

$$i = \frac{2nFSc_{M^+_{solution}} K_{pt}\gamma_{M^+} D_{M^+_{solid}}^{1/2}}{(\gamma_{M^+} + K_{pt})(\pi t)^{1/2}} \sum_{j=0}^{\infty}\left(\frac{1 - K_{pt}/\gamma_{M^+}}{1 + K_{pt}/\gamma_{M^+}}\right)^j \exp[-(j+1/2)^2\delta^2/D_{M^+_{solid}}t] \quad (23)$$

dx.doi.org/10.1021/jp308966w | J. Phys. Chem. C 2012, 116, 25977−25983

Here S is the exposed area of the solid film and $\gamma_{M^+} = (D_{M^+_{solution}}/D_{M^+_{solid}})^{1/2}$. At infinite times, this equation should tend to a Cottrell diffusion of cations in the electrolyte phase.[53]

Additionally, it will be assumed that a binding reaction between the immobile redox centers and the cations, equivalent to the process represented by eq 7, takes place in the solid, as proposed by Wu et al.[54] for the protonation processes in redox polymers. Now eq 15 must be replaced by:

$$D_{M^+_{solid}}\left(\frac{\partial^2 c_{M^+_{solid}}(z,t)}{\partial x^2}\right) = \frac{\partial c_{M^+_{solid}}(z,t)}{\partial t} \pm \frac{\partial c_{LM}(z,t)}{\partial t}, \quad 0 < z < \delta \tag{24}$$

Where $c_{LM}(z,t)$ represents the concentration of the cation−redox center adduct, LM. The sign between the two terms in the above equation is + for reduction with cation insertion and is also + for oxidation with anion insertion into the film. Within the solid film, mass balance for L yields:

$$c_L = c_L(z,t) + c_{LM}(z,t) = c_L(\delta,t) + c_{LM}(\delta,t) \tag{25}$$

where $c_L(\delta,t)$ and $c_{LM}(\delta,t)$ are, respectively, the concentrations of L and LM in the solid at the electrolyte/solid film interface and c_L is the initial concentration of immobile redox centers homogeneously distributed within the solid.

If the binding reaction is faster than diffusion in the crystal, then one can assume that chemical equilibrium is established at all points within the solid and:

$$K_{bd} = \frac{c_{LM}(z,t)}{c_{M^+_{solid}}(z,t)c_L(z,t)} = \frac{c_{LM}(\delta,t)}{c_{M^+_{solid}}(\delta,t)c_L(\delta,t)} \tag{26}$$

where K_{bd} is the binding equilibrium constant. Combining eqs 25 and 26, one can arrive to the following expressions for the effective concentration of L and LM:

$$c_L(z,t) = \frac{c_L(\delta,t)[1 + K_{bd}c_{M^+_{solid}}(\delta,t)]}{1 + K_{bd}c_{M^+_{solid}}(z,t)} \tag{27}$$

$$c_{LM}(z,t) = \frac{K_{bd}c_{M^+_{solid}}(z,t)c_L(\delta,t)[1 + K_{bd}c_{M^+_{solid}}(\delta,t)]}{1 + K_{bd}c_{M^+_{solid}}(z,t)} \tag{28}$$

Introducing the derivative of eq 28 with respect to time into eq 24 yields:

$$D_{M^+_{solid}}\left(\frac{\partial^2 c_{M^+_{solid}}(z,t)}{\partial z^2}\right) = \frac{\partial c_{M^+_{solid}}(z,t)}{\partial t} \times \left[1 + \frac{K_{bd}c_L(\delta,t)[1 + K_{bd}c_{M^+_{solid}}(\delta,t)]}{1 + K_{bd}c_{M^+_{solid}}(z,t)} - \frac{K_{bd}{}^2 c_{M^+_{solid}}(z,t)c_L(\delta,t)(1 + K_{bd}c_{M^+_{solid}}(\delta,t))}{(1 + K_{bd}c_{M^+_{solid}}(z,t))^2}\right] \tag{29}$$

For short-time experiments ($c_{M^+_{solution}}(z,t) \to 0$ when $t \to 0$), or at any times when K_{bd} is low, the above equation reduces to:

$$D_{M^+_{solid}}\left(\frac{\partial^2 c_{M^+_{solid}}(z,t)}{\partial z^2}\right) = \frac{\partial c_{M^+_{solid}}(z,t)}{\partial t}[1 + K_{bd}c_L(\delta,t)(1 + K_{bd}c_{M^+_{solid}}(\delta,t))] \tag{30}$$

Considering that, at short times, $c_L(\delta,t)$ tends to c_L and $c_{M^+_{solid}}(\delta,t)$ tends to $c_{M^+_{solution}}$, eq 30 can be regarded as equivalent to eq 24, replacing $D_{M^+_{solid}}$ by an effective diffusion coefficient, $D^{eff}_{M^+_{solid}}$, that can be taken as:

$$D^{eff}_{M^+_{solid}} = \frac{D_{M^+_{solid}}}{1 + K_{bd}c_L[1 + K_{bd}K_{pt}c_{M^+_{solution}}]} \tag{31}$$

As a result, eq 23 can be replaced by:

$$i = \frac{2nFSc_{M^+_{solution}}K_{pt}\gamma^{eff}_{M^+}(D^{eff}_{M^+_{solid}})^{1/2}}{(\gamma^{eff}_{M^+} + K_{pt})(\pi t)^{1/2}} \sum_{j=0}^{\infty}\left(\frac{1 - K_{pt}/\gamma^{eff}_{M^+}}{1 + K_{pt}/\gamma^{eff}_{M^+}}\right)^j \exp[-(j + 1/2)^2\delta^2/D^{eff}_{M^+_{solid}}t] \tag{32}$$

where $\gamma^{eff}_{M^+} = (D_{M^+_{solution}}/D^{eff}_{M^+_{solid}})^{1/2}$. This behavior can be expected at relatively long times in the chronoamperometric experiments performed in relatively high concentrations of electrolyte, thus favoring the attainment of the equilibrium condition expressed by eq 26.

At relatively long times, a Cottrell-like behavior is predicted, the product $it^{1/2}$ tending to a limiting value given by:

$$(it^{1/2})_{lim} = \frac{2nFSc_{M^+_{solution}}K_{pt}(D_{M^+_{solution}})^{1/2}}{(\gamma^{eff}_{M^+} + K_{pt})\pi^{1/2}} \tag{33}$$

Using this approach, the values of the equilibrium constants K_{bd} and K_{pt}, can be estimated from current/time CA data provided that the concentration of immobile redox centers in the solid and the diffusion coefficients for the M^+ ions in the solution and in the solid are known. This treatment could be simplified in two cases. First, when $\gamma^{eff}_{M^+_{solid}} \ll K_{pt}$, eq 33 reduces to:

$$(it^{1/2})_{lim} \approx \frac{2nFAc_{M^+_{solution}}(D_{M^+_{solution}})^{1/2}}{\pi^{1/2}} \tag{34}$$

Second, when $\gamma^{eff}_{M^+_{solid}} \gg K_{pt}$, eq 33 can be approached by:

$$(it^{1/2})_{lim} \approx \frac{2nFAc_{M^+_{solution}}K_{pt}(D_{M^+_{solution}})^{1/2}}{\pi^{1/2}[1 + K_{bd}c_L(1 + K_{pt}K_{bd}c_{M^+_{solution}})]^{1/2}} \tag{35}$$

Thermochemical Considerations: The Activity Problem. Figure 5 shows a thermochemical cycle where the processes described by eqs 3−7 are mutually interrelated. From this cycle, one can write:

$$\Delta G^{\ominus}_{el} = \Delta G^{\ominus}_{e} + \Delta G^{\ominus}_{ret}(L) - \Delta G^{\ominus}_{ret}(ML) + n\Delta G^{\ominus}_{solv}(M^+) + n\Sigma_e \tag{36}$$

Here $\Delta G^{\ominus}_{ret}(L)$ and $\Delta G^{\ominus}_{ret}(LM)$ denoted the reticular Gibbs energies associated with the formation of the L and ML crystals from their individual components in the gas phase. Notice that, as in the case of the solution phase $BBCr^+/BBCr$ system, an

dx.doi.org/10.1021/jp308966w | J. Phys. Chem. C 2012, 116, 25977−25983

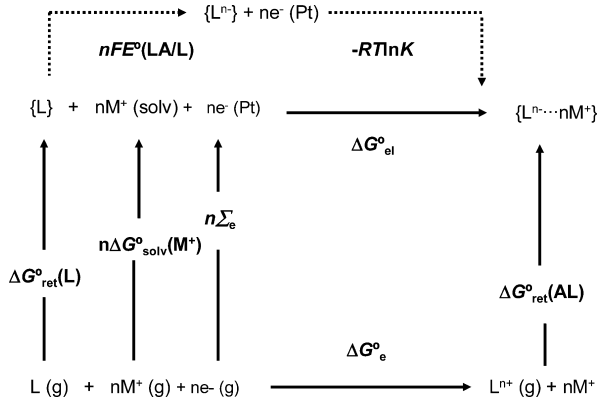

Figure 5. Thermochemical cycle for the cation-assisted reduction of an ion-insertion solid L using a Pt base electrode.

"uncompensated" solvation Gibbs energy term appears. Accordingly, only the partial electron-transfer process described by eq 6 would be solvent-independent. The solvent-independent redox potential $E^{\ominus}_{L^{m+}/(m-n)+}$ could be calculated under voltammetric conditions from the voltammetric midpeak potentials provided that the equilibrium constant of the partial process described by eq 7 and the thermochemical activities of the oxidized and reduced forms of the solid and M^+ ions in the electrolyte bulk could be estimated as:

$$E^{\ominus}(\mathrm{LM/L}) = E_{\mathrm{mp}}(\mathrm{LM/L}) - \frac{RT}{nF}\ln K - \frac{RT}{nF}\ln\left(\frac{a_{\mathrm{LM}}}{a_{\mathrm{L}}}\right) - \frac{RT}{F}\ln a_{\mathrm{M}^+_{\mathrm{solution}}} \quad (37)$$

In principle, K could be estimated as described in the precedent section, while $a_{\mathrm{M}^+_{\mathrm{solution}}}$ could be obtained from experimental E_{mp} versus log $a_{\mathrm{M}^+_{\mathrm{solution}}}$ plots assuming that the coefficients of activity tends to unit at low concentrations, as already described.[41−43]

The estimate of the thermodynamic activities of the oxidized and reduced forms of the solid, however, is problematic. In principle, the advance of the electrochemical process involves the permeation of the pristine solid, L, by the electrolyte cations, M^+. This can result in the formation of mixed crystals where the thermodynamic activities of the solid species can be taken as proportional to their molar fractions.[61] It is conceivable, however, that both the mother and daughter solid compounds segregate so that the reduced solid would appear as inclusions in the oxidized solid, making both phases accessible to electrochemical inputs, as described by Hermes et al.[62] for Prussian blue−type metal hexacyanoferrates. In this second case, the thermodynamical activities of the components, a_{LM} and a_{L}, should be considered as a unit. In several instances, however, the formation of bilayered structures has been reported.[63,64] Obviously, experimental testing is needed with this regard. On first examination, the aforementioned Prussian blue[41] and alkynyl−diphosphine dinuclear Au(I) complexes and heterometallic Au(I)−Cu(I) cluster complexes containing ferrocenyl units[42,43] could be plausible solids usable as solvent-independent redox systems. Among others, possible candidates could also be hybrid inorganic−organic materials consisting of electroactive species entrapped into inert supports such as zeolites[57,65] or Maya Blue.[66−68] Interestingly, the use of different L, S, and so on systems could be used to test the self-consistency of the proposed approach: constant $E^{\ominus}_{L^{m+}/L^{(m-n)+}} - E^{\ominus}_{S^{m+}S^{(m-n)+}}$ differences should be obtained regardless the solvent.

CONCLUSIONS

Using the Lovric and Scholz modeling for the electrochemistry of ion insertion solids, a formally solvent-independent redox system can be defined under voltammetric conditions using the VMP approach. The redox potential for this partial process could be estimated from voltammetric and chronoamperometric data assuming electrochemical reversibility and diffusive charge transport in the solution and solid phases on the basis of the Nernst equation and Ficks' laws and accounts of electrolyte/solid partition and ion binding equilibria. Although the proposed theoretical approach involves two extrathermodynamic assumptions (absence of net charge accumulation in the solid complex/electrolyte boundary and maintenance of the structure of the solid and the ion binding regardless the solvent), it could provide a potentially interesting way to define solvent-independent redox scales.

AUTHOR INFORMATION

Corresponding Author

*E-mail: antonio.domenech@uv.es.

Notes

The authors declare no competing financial interest.

ACKNOWLEDGMENTS

The author wishes to thank Profs. Fritz Scholz and Milivoj Lovric for their help in revising the manuscript. Financial support is gratefully acknowledged from the MEC Project CTQ2011-28079-CO3-02, which is supported with ERDF funds.

REFERENCES

(1) Trasatti, S. *Pure Appl. Chem.* **1986**, *59*, 955−966.
(2) Bjerrum, N.; Larsson, E. *Z. Phys. Chem.* **1927**, *127*, 358−384.
(3) Kolthoff, I. M. *Pure Appl. Chem.* **1971**, *25*, 305−325.
(4) Gritzner, G. *Electrochim. Acta* **1998**, *44*, 73−83.
(5) Donald, W. A.; Leib, R. D.; O'Brien, J. T.; Bush, M. F.; Williams, E. R. *J. Am. Chem. Soc.* **2008**, *130*, 3371−3381.
(6) Donald, W. A.; Leib, R. D.; O'Brien, J. T.; Williams, E. R. *Chem.—Eur. J.* **2009**, *15*, 5926−5934.
(7) Donald, W. A.; Leib, R. D.; Demireva, M.; O'Brien, J. T.; Prell, J. R.; Williams, E. R. *J. Am. Chem. Soc.* **2009**, *131*, 13328−13337.
(8) Isse, A. A.; Gennaro, A. *J. Phys. Chem. B* **2010**, *114*, 7894−7899.
(9) Cox, B. G.; Parker, A. J.; Waghorne, W. E. *J. Am. Chem. Soc.* **1973**, *95*, 1010−1014.
(10) Alexander, R.; Parker, A. *J. Am. Chem. Soc.* **1967**, *89*, 5549−5551.
(11) Popovych, O.; Dill, A. J. *Anal. Chem.* **1969**, *41*, 456−462.
(12) Gritzner, G.; Kuta, J. *Pure Appl. Chem.* **1984**, *56*, 461−466.
(13) Gritzner, G. *Pure Appl. Chem.* **1990**, *62*, 1839−1858.
(14) Rose, D.; Benjamin, I. *J. Phys. Chem. B* **2009**, *113*, 9296−9303.
(15) Tissandier, M. D.; Cowen, K. A.; Feng, W. Y.; Gundlach, E.; Cohen, M. H.; Earhart, A. D.; Coe, J. V. *J. Phys. Chem. A* **1998**, *102*, 7787−7794.
(16) Tawa, G. J.; Topol, I. A.; Burk, S. K.; Rashin, A. A. *J. Chem. Phys.* **1998**, *109*, 4852−4863.
(17) Topol, I. A.; Tawa, G. J.; Burk, S. K.; Caldwell, R. A.; Rashin, A. A. *J. Chem. Phys.* **1999**, *111*, 10998−11014.
(18) Mejias, J. A.; Lago, S. *J. Chem. Phys.* **2000**, *113*, 7306−7316.
(19) Zhan, C.-G.; Dixon, D. A. *J. Phys. Chem. A* **2001**, *105*, 11534−11540.
(20) Zheng, F.; Zhan, C.-G.; Ornstein, R. L. *J. Phys. Chem. B* **2002**, *106*, 717−722.

(21) Pliego, J. R., Jr; Riveros, J. M. *Phys. Chem. Chem. Phys.* **2002**, *4*, 1622−1627.
(22) Zhan, C.-G.; Dixon, D. A.; Sabri, M. I.; Kim, M.-S.; Spencer, P. S. *J. Am. Chem. Soc.* **2002**, *124*, 2744−2752.
(23) Zhan, C.-G.; Dixon, D. A. *J. Phys. Chem. A* **2004**, *108*, 2020−2029.
(24) Ahlquist, M.; Kozuch, S.; Shaik, S.; Tanner, D.; Norrby, P.-O. *Organometallics* **2006**, *25*, 45−47.
(25) Kelly, C. P.; Cramer, C. J.; Truhlar, D. G. *J. Phys. Chem. B* **2007**, *111*, 408−422.
(26) Samec, Z. *Pure Appl. Chem.* **2004**, *76*, 2147−2180.
(27) Dryfe, R.. A. W. *Phys. Chem. Chem. Phys.* **2006**, *8*, 1869−1883.
(28) Langmaier, J.; Samec, Z. *Electrochem. Commun.* **2007**, *9*, 2633−2638.
(29) Sherburn, A.; Platt, M.; Arrigan, D. W. M.; Boag, N. M.; Dryfe, R. A. W. *Analyst* **2003**, *128*, 1187−1192.
(30) Josserand, J.; Lagger, G.; Jensen, H.; Ferrigno, R.; Girault, H. H. *J. Electroanal. Chem.* **2003**, *546*, 1−13.
(31) Sun, P.; Laforge, F. O.; Mirkin, M. V. *Phys. Chem. Chem. Phys.* **2007**, *9*, 802−823.
(32) Sun, P.; Laforge, F. O.; Mirkin, M. V. *J. Am. Chem. Soc.* **2007**, *129*, 12410−12411.
(33) Olaya, A. J.; Méndez, M. A.; Cortes-Salazar, F.; Girault, H. H. *J. Electroanal. Chem.* **2010**, *644*, 60−66.
(34) Gulaboski, R.; Scholz, F. *J. Phys. Chem. B* **2003**, *107*, 5650−5657.
(35) Scholz, F. *Annu. Rep. Prog. Chem., Sect. C* **2006**, *102*, 43−70.
(36) Marken, F.; McKenzie, K. J.; Shul, G.; Opallo, M. *Faraday Discuss.* **2005**, *129*, 219−229.
(37) MacDonald, S. M.; Opallo, M.; Klamt, A.; Eckert, F.; Marken, F. *Phys. Chem. Chem. Phys.* **2008**, *10*, 3925−3933.
(38) Gulaboski, R.; Caban, K.; Stojek, Z.; Scholz, F. *Electrochem. Commun.* **2004**, *6*, 215−218.
(39) Scholz, F.; Meyer, B. In *Electroanalytical Chemistry, A Series of Advances*; Bard, A. J., Rubinstein, I., Eds.; Marcel Dekker: New York: 1998; Vol. *20*, pp 1−86.
(40) Scholz, F.; Schröder, U.; Gulaboski, R. *Electrochemistry of Immobilized Particles and Droplets*; Springer: Berlin-Heidelberg, 2005.
(41) Doménech, A.; Montoya, N.; Scholz, F. *J. Electroanal. Chem.* **2011**, *657*, 117−122.
(42) Doménech, A.; Koshevoy, I. O.; Montoya, N.; Pakkanen, T. A. *Electrochem. Commun.* **2011**, *13*, 96−98.
(43) Doménech, A.; Koshevoy, I. O.; Montoya, N.; Karttunen, A. J.; Pakkanen, T. A. *J. Chem. Eng. Data* **2011**, *56*, 4577−4586.
(44) Bond, A. M.; Fletcher, S.; Marken, F.; Shaw, S. J.; Symons, P. J. *J. Chem. Soc. Faraday Trans.* **1996**, *92*, 3925−3933.
(45) Lovric, M.; Scholz, F. *J. Solid State Electrochem.* **1997**, *1*, 108−113.
(46) Lovric, M.; Hermes, M.; Scholz, F. *J. Solid State Electrochem.* **1998**, *2*, 401−404.
(47) Oldham, K. B. *J. Solid State Electrochem.* **1998**, *2*, 367−377.
(48) Lovric, M.; Scholz, F. *J. Solid State Electrochem.* **1999**, *3*, 172−175.
(49) Schröder, U.; Oldham, K. B.; Myland, J. C.; Mahon, P. J.; Scholz, F. *J. Solid State Electrochem.* **2000**, *4*, 314−324.
(50) Andrieux, C. P.; Savéant, J.-M. *J. Electroanal. Chem.* **1982**, *142*, 1−30.
(51) Laviron, E. *J. Electroanal. Chem.* **1980**, *112*, 1−9.
(52) Weppner, W. Electrode Performance. In *Solid State Electrochemistry*; Bruce, P. G., Ed.; Cambridge Univ. Press: Cambridge, U.K., 1995; pp 199−228.
(53) White, H. S.; Leddy, J.; Bard, A. J. *J. Am. Chem. Soc.* **1982**, *104*, 4811−4817.
(54) Wu, X. Z.; Kitamori, T.; Sawada, T. *J. Phys. Chem.* **1992**, *96*, 9406−9410.
(55) Baucke, F. G. K. *Phys. Chem. Glasses* **2001**, *42*, 220−225.
(56) Scholz, F. *J. Solid State Electrochem.* **2011**, *15*, 67−68.
(57) Scholz, F.; Lovric, M.; Stojek, Z. *J. Solid State Electrochem.* **1997**, *1*, 134−142.
(58) Hermes, M.; Scholz, F. In *Solid State Electrochemistry I*; Kharton, V. V., Ed.; Wiley-VCH: Weinheim, Germany, 2009; pp 179−226.
(59) Scholz, F. *Electroanalytical Methods*, 2nd ed.; Springer: Berlin-Heidelberg, 2010; p 22.
(60) Doménech, A. *J. Phys. Chem. B.* **2004**, *108*, 20471−20478.
(61) Jaworsky, A.; Stojek, Z.; Scholz, F. *J. Electroanal. Chem.* **1993**, *354*, 1−9.
(62) Hermes, M.; Lovric, M.; Hartl, M.; Retter, U.; Scholz, F. *J. Electroanal. Chem.* **2001**, *501*, 193−204.
(63) Pickup, P. G.; Leidner, C. R.; Denisevich, P.; Willman, K. W.; Muray, R. W. J. *Electroanal. Chem.* **1984**, *164*, 39−61.
(64) Leidner, C. P.; Denisevich, P.; Willman, K. W.; Murray, R. W. *J. Electroanal. Chem.* **1984**, *164*, 63−78.
(65) Doménech, A.; Formentín, P.; García, H.; Sabater, M. J. *J. Phys. Chem. B* **2002**, *106*, 574−582.
(66) Doménech, A.; Doménech, M. T.; Vázquez de Agredos, M. L. *J. Phys. Chem. B* **2006**, *110*, 6027−6039.
(67) Doménech, A.; Doménech, M. T.; Sánchez del Río, M.; Vázquez de Agredos, M. L. *J. Solid State Electrochem.* **2009**, *13*, 869−878.
(68) Doménech, A.; Doménech, M. T.; Sánchez del Río, M.; Goberna, S.; Lima, E. *J. Phys. Chem. C* **2009**, *113*, 12118−12131.